UHF Acoustic Microscopic Imaging of Resonator Motion

Ken L. Telschow*, Vance A. Deason and David L. Cottle
Idaho National Engineering and Environmental Laboratory
Idaho Falls, ID 83415-2209, USA

John D. Larson III †
Agilent Technology Laboratories
3500 Deer Creek Road, Mail Stop 26M-2
Palo Alto, CA 94304-1392, USA

Abstract - An important characteristic of acoustic resonator design at ultra high frequencies (UHF) is the efficiency of the device, which is affected by leakage radiation beyond the active transducer area. In order to directly measure leakage radiation, acoustic microscopic imaging of the ultrasonic resonant motion at 880 MHz has been performed with an autocompensating interferometer and heterodyne demodulation. A method of interferometric detection based on two-wave mixing in a photorefractive material was employed to allow for automatic quadrature detection and compensation of low frequency vibrational effects. Heterodyne phase modulation was used to produce a beat frequency of 25 kHz to allow for narrowband detection utilizing lock-in amplifier techniques. A sensitivity of 5×10^{-5} nm was obtained with a 10 sec time constant and detection light power of about 0.5 mW. Over 90 dB dynamic drive range was recorded at the UHF operating frequency without vibration isolation of the microscope or optics. The method of calibration and results of scanning measurements on various resonators are presented and discussed in connection with current limitations and future improvements.

I. INTRODUCTION

UHF ultrasonic resonators are being developed for specialized signal processing by the telecommunication industry. Operation is now being performed at 1-2 GHz and higher frequencies are contemplated for the future. Very small dimensions are needed to achieve these ultra high frequencies as well as satisfy other telecommunication requirements. In order to optimize the development, operation, and manufacture of these resonators, knowledge of the ultrasonic leakage from the device is important. This paper describes an optical method for determining leakage by direct measurement beyond the active transducer area.

II. DYNAMIC HOLOGRAPHIC DETECTION

A new approach to optical detection of ultrasonic motion in a microscopic geometry has been developed using photorefractive materials [1]. Two-wave mixing of a signal and reference beam within these materials can produce an output beam that demodulates the phase difference into an intensity variation. This method is similar to many interferometric techniques for phase demodulation of ultrasonic motion [2] except that active stabilization between the two beam paths at the phase quadrature point is not required. The photorefractive approach automatically produces a quadrature phase shift between signal and reference beams when the charge transport mechanism is diffusive [3]. Another advantage is that complicated optical wavefronts from surfaces with rough features are readily accommodated through the volume holographic process to produce the optimum reference beam for interferometric detection (i.e. samples with rough surfaces can be investigated with little loss of sensitivity due to speckle averaging). Finally, the ultimate goal of these measurements is to obtain images of ultrasonic motion over the entire surface

within a single video frame, not requiring scanning over the surface. This has been accomplished at MHz frequencies on surfaces from 1"x 1" to 6"x 6" for both resonant and traveling wave motion [4,5].

A schematic of the optical detection process is shown in Figure 1. A single frequency laser at 532 nm produces both the signal and reference beams. After suitable polarization rotation and reflection from polarized beam splitters, the two beams are combined in a Bismuth Silicon Oxide (BSO) photorefractive crystal. The resultant output beam from the two-wave mixing is then measured with a photodiode detector and lock-in amplifier.
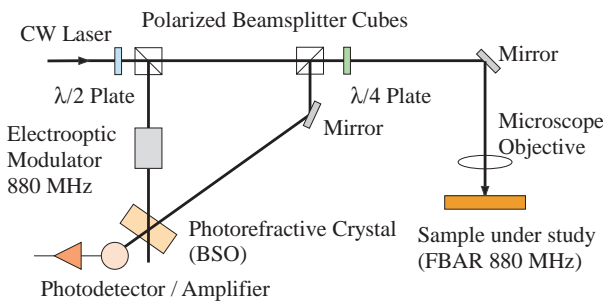

Figure 1: Narrowband Optical Detection Schematic.

III. CALIBRATION

The out-of-plane motion of a vibrating surface produces a phase shift of an optical beam reflected normal to the surface of $\varphi_S(t) = \frac{4\pi\xi}{\lambda}$, where $\xi(t) = \xi_0 \cos(2\pi f t + \psi)$ and λ is the optical wavelength. Combining this beam with a reference beam phase modulated in a similar manner at the offset frequency $f + \Delta f$, produces an interference pattern with a narrowband component varying at the frequency Δf. Two-wave mixing within the photorefractive material produces an output beam with intensity of this component [6] of:

$$\left| I_{AC} \right| \propto J_0(\varphi_S) J_1(\varphi_S) J_0(\varphi_R) J_1(\varphi_R) \qquad (1)$$

with φ_S, φ_R the optical phase modulation depth on the signal and reference beams. It is apparent that both the signal and reference beam modulations

produce an output intensity proportional to the product of the 0th and 1st order Bessel functions. This particular Bessel function product has a maximum value for a modulation depth of $\delta = 1.08$ radians and is proportional to δ for smaller modulations. At an optical wavelength of 532 nm, this maximum value corresponds to an ultrasonic displacement of 45.8 nm. Figure 2 shows the results of measuring this response by driving the
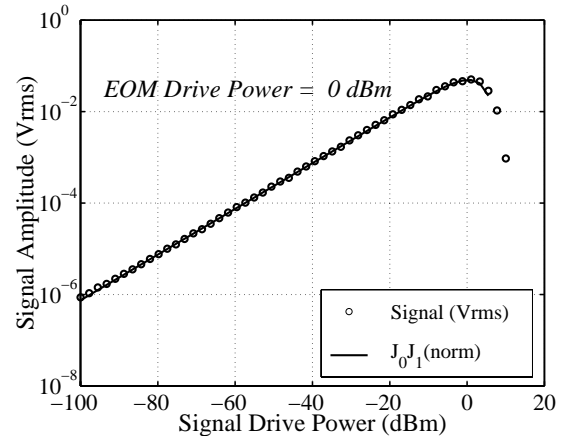

Figure 2: Calibration Phase Measurement

electro-optic modulator (EOM) as a function of amplitude at fixed frequency. Maximum phase modulation depth occurs at an input drive power to the amplifier/splitter chain, of about 0 dBm for the amplifier and modulator used. This resulted in a power of about 1 Watt delivered to the EOM, which was matched to 50 Ohms at 880 MHz. The solid line in Figure 2 shows the expected Bessel function product.

The achievement of the maximum phase modulation provided a simple means of calibration with three phase locked generators, two UHF generators for the signal and EOM modulations and a low frequency generator to produce the difference frequency. For calibration, the two signals were combined on the EOM and the resultant signal phase shift was recorded with fixed drive power on the EOM. The result agreed very well with equation (1) as shown in Figure 2.

The FBAR resonator is a micromachined membrane of Aluminum Nitride (AlN) with acoustically thin refractory metal electrodes, designed to resonate at ~ 900 MHz. It is grown on a silicon wafer for support at the edges.

In operation, it vibrates in the plate thickness mode and exhibits an electro-acoustical coupling $k_t^2 \sim 5\%$. It presents a highly reactive load to the driver amplifier. Figure 3 illustrates the magnitude of impedance vs. frequency for an FBAR of dimensions $\sim$ 200 by 150 microns (μm). For operation at 880 MHz, the FBAR presented an impedance of 3.2 +j27 Ohms, resulting in a mismatch loss of $\sim$ -7 dB relative to driving a 50 Ohm load. This means that the net power actually driving the FBAR is somewhat reduced, compared to that driving the EOM, for the same amplifier input drive power.
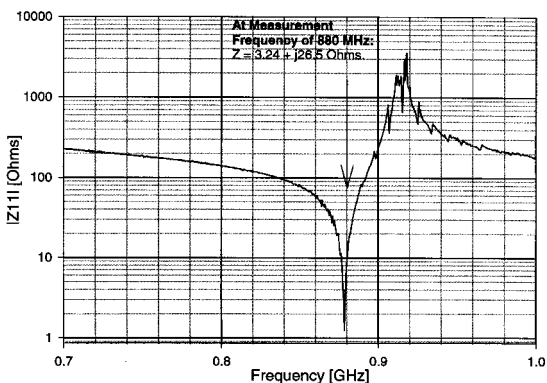

Figure 4: Ultrasonic Displacement Amplitude

5×10^{-5} nm was obtained with a 10 second time constant, photodiode quantum efficiency of 70% and detection light power of about 0.5 mW. Shot noise limited phase detection is determined by

$$\Phi_{min} = \sqrt{\frac{2hc\Delta f}{\lambda \eta P_0}} \qquad (2)$$

for h Planck's constant, c the speed of light, η the photodetector quantum efficiency, and P_0 the average optical intensity on the detector. This calculation yields a minimum detectable phase shift of 1.5×10^{-7} radians and corresponding displacement of about 6.2×10^{-6} nm for the parameters listed. This suggests that the measured displacements were still about 1 order of magnitude above the theoretical shot noise limit and that further improvement is possible.

Figure 4 illustrates a y-axis scan along a line from the center to the edge of the active FBAR, and continuing about 300 μm further along the inactive silicon region. This shows that the energy is well confined to the active region of the FBAR resonator, but the excellent dynamic range of the instrument allows the low level of acoustical leakage off the FBAR to be measured.

Figure 3 : Measured Magnitude of Input Impedance to FBAR Resonator.

IV. UHF MEASUREMENTS

Once the EOM drive power was set for maximum response, the signal phase shift resulting from excitation of the FBAR was recorded and compared to that produced in the calibration measurement. The measured voltage amplitude was then converted to ultrasonic displacement using the known functional dependence of equation (1). The results of calibration and measurement on a particular FBAR are shown in Figure 4. The right shift in the measured data along the Drive Power axis is, in part, due to the mismatch of the FBAR mentioned above.

A maximum ultrasonic displacement of about 3.4 nm @ 880 MHz was obtained. A dynamic range of about 5 orders of magnitude was found with the present noise levels. A sensitivity of
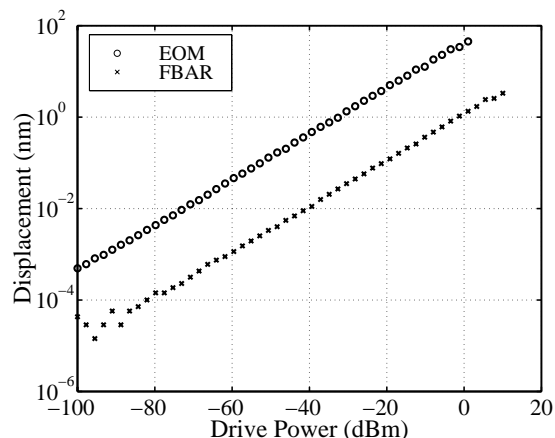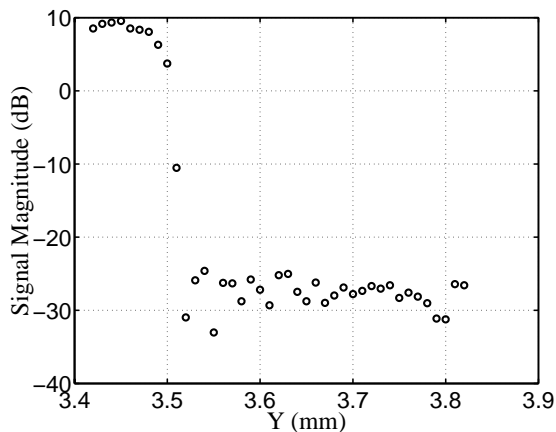
Figure 4 FBAR Resonator Surface Displacement, Y-Axis Scan, Center to Edge of Die.

ξ_{max}=2.58 (nm) [0 dB]

Figure 5: FBAR Resonator Amplitude Distribution

A complete mapping of the ultrasonic displacement over the surface of the resonator and in the area adjacent to the resonator, was obtained by raster scanning the detection beam (spot size about 4μm) across the entire active FBAR resonator surface, and a few microns off the edges. Figure 5 shows the results for the particular FBAR under investigation. The resonator itself exhibited a fairly uniform response of about 2.5 nm surface displacement amplitude over the active surface. From the inactive areas nearby, the leakage was determined to be ~40 dB down from that of the maximum surface amplitude. Clearly, these measurements can be very helpful for determining the ultrasonic properties of very small UHF resonators in-situ to their operational environment.

V. ACKNOWLEDGEMENTS

[1] P. Yeh, *Introduction to Photorefractive Nonlinear Optics*, (John Wiley, New York, 1993).

[2] J. W. Wagner, "Optical Detection of Ultrasound," *Physical Acoustics*, Vol. XIX, Eds. Thurston, R. N., and Pierce, A.D., (Academic Press, NY, 1990) Chp. 5.

[3] R. K. Ing and J. P. Monchalin, "Broadband optical detection of ultrasound by two-wave mixing in a photorefractive crystal," Appl. Phys. Lett. 59, 3,233 (1991).

[4] T. C. Hale, K. L. Telschow, and V. A. Deason, "Photorefractive optical lock-in vibration spectral measurement," Applied Optics, 111, 8,248–8,258 (1997).

[5] K.L. Telschow, V. A. Deason, R. S. Schley and S. M. Watson, "Direct Imaging of Lamb Waves in Plates using Photorefractive Dynamic Holography," J.Acoust. Soc. Am. 106(5), 2578-2587 (1999).

[6] K.L. Telschow, V. A. Deason, K.L. Ricks and R. S. Schley, "Photorefractive laser ultrasound spectroscopy for materials characterization," *Nondestructive Characterization of Materials VIII,* ed. R. E. Green, Jr., (Plenum Press, New York, 1998) 79-84.

*   Ken Telschow: telsch@inel.gov

†   John Larson: john_larson@agilent.com